International Journal of Material Forming (2024) 17:42
https://doi.org/10.1007/s12289-024-01841-z

ORIGINAL RESEARCH

The Comparison between Additively Manufactured and Molded 3D Scaffolds for Tissue Engineering Applications

Tijana Kavrakova[1] · **Luciano Vidal**[1] · **Jean-Yves Hascoet**[1]

Received: 28 May 2024 / Accepted: 3 June 2024 / Published online: 1 July 2024

Abstract

Blood vessels are essential as they transport oxygen and nutrients. To address the increasing mortality rate from cardiovascular diseases, modern science is focusing on clinical trials for replacing human blood vessels with artificial ones. However, the challenge lies in replicating the intricate anatomy with exact dimensional accuracy on a small scale. This work concentrates on developing innovative fabrication solutions in tissue engineering 3D scaffolds. The study captured two prototypes; one based on traditional manufacturing and the other applied an additive manufacturing principle. Once single-layered construct were manufactured, the results were evaluated in terms of dimensional accuracy measuring the constructs' length, diameter and thickness. Additional tests were performed for finding the strain at break by applying manual strain-induced method. The samples demonstrated that molding excelled in terms of precision however, the mechanical performance did not meet the ISO 7198 standard. Additive manufacturing approach on the other hand, fully satisfied the structural criteria yet the obtained thickness significantly varied from the given one. Furthermore, efforts were made for fabricating three-layered scaffolds and while AM approach brought preferable results, difficulties were faced with molding. Thus, the importance of this work lies in demonstrating the process capabilities of two methods. The results indicate that while AM is suitable for fabricating multilayered constructs with good structural integrity, molding appears promising for small diameter scaffolds, as it can reduce the anatomical mismatches. Therefore, future work will focus on improving the limitations of these methods for developing three-layered vascular grafts within the admissible dimensional and mechanical criteria.

Keywords Additive manufacturing · Bioprinting · Biofabrication · Vascular constructs

Introduction

Cardiovascular diseases are the number one killer in the world. Current data show that 550 million people live with damage to the circulatory system. World Health Organization (WHO) estimates that in 2019 17.1 million people were killed due to CVD [1]. The number corresponds to 32% of global deaths and the term itself grasps a wide range of diseases, such as ischemic heart diseases, ischemic or hemorrhagic strokes, heart valve damage, aneurysm, etc. [2]. Despite this broad spectrum, the deadliest of all are ischemic heart disease and strokes with 85% of the overall mortality [3]. Another name of the first mentioned is coronary artery diseases (CAD) that appear due to the build-up of cholesterol on the arterial walls and thus, obstruct the delivery of the oxygenated blood from the heart to the organs, resulting in myocardial infarction i.e. a heart attack. Strokes involve clots in the blood vessels, affecting the brain's circulation. Current treatments include vascular grafts, such as stents and bypasses for CAD and endovascular thrombectomy for strokes. However, these treatments come with some risks, as it often occurs that patient's body rejects the stent, or develops an allergic reaction. By passes on the other hand, offer a more autologous approach, yet, threats come due to the open heart surgery and long recovery. Actions for strokes also involve surgeries with a high success rate of 85%, but they can damage the blood vessel, infection or death due to excessive bleeding. Therefore, current research focuses on developing promising solutions for minimizing the risks and maximizing the success rate.

✉ Jean-Yves Hascoet
jean-yves.hascoet@ec-nantes.fr

Tijana Kavrakova
Tijana.Kavrakova@ec-nantes.fr

[1] UMR 6183, Nantes Université, Ecole Centrale Nantes, CNRS, 44000] Nantes, GeM, France

Tissue engineering is a multidisciplinary field that aims to restore, sustain or enhance tissue functionality. The discipline itself exists since the nineteenth century [4], however it was not until the appearance of bio-printing that it took a significant turn. The application of AM in medical sector had a vast impact to the shift of 2D dimensional models into 3D space. Cultured environments used for drug testing and disease modelling were replaced with more realistic 3D models. This remarkable discovery did not only provide with more reliable data, but as well as opened the door to other applications, such as tissue/organ replacements.

Now-a-days, one aspect of this field is concentrated on CVD. There have been efforts to create an autologous grafts that will minimize the risks of bleeding, immune response and death. One can produce a successful vascular transplant by first, mimicking the complex blood vessel anatomy of three morphologically distinct layers and then replicating the blood vessel function. However, the difficulty lies in the limited machine capacity to mimic the blood vessel anatomy on such a small scale. These constraints can thus, cause anatomical mismatches between the artificial and the human vessel [5]. Additionally, the constrained cells interactions between layers results with graft malfunction. Hence, current research is focusing on developing techniques and methodologies to minimize dimensional disparities while enhancing cell interactions to improve vascularization.

Ongoing research is mostly focused on the application of AM in tissue engineering blood vessels. While some are studying the properties of the material to predict and optimize the process, others are focusing on development of innovative techniques. For instance Bom et al. present a comprehensive review that explains the link between the rheology and the printability, extrudability, accuracy, shape fidelity [6]. Similarly, in the paper of Naghieh et al. the printability is related to pore size and strand diameter. They concluded that the result is a function of printing parameters, swelling, material concentration and degradation [7]. Kang et al. made efforts to understand the effect of extrusion parameters on print accuracy and cell viability. Accuracy was measured by proposing dimensionless variable indices of width, height and length that demonstrated the change of the dimensions over the total length and height. Additionally, cell viability was assessed by postulating a Newtonian viscosity and finding the admissible shear stress that will promote tissue development [8]. In contrast to this, recent studies focus on the non-Newtonian models for materials used in extrusion based bio printing. For instance, Kokol et al. developed a rheological study on the phase change of different gelatin concentrations that provide improved data and promote cell adhesion [9]. Another study that focused on the deposition uniformity was the one of Soltan et al. where they presented the print error by finding the ratio of the experimental and the theoretical length [10].

Other aspect is focused on proposing new solutions that will surpass the challenges with material manipulation due to phase change, machine capacity and improve layer interactions. For instance, Xu et al. have developed an Integrated Tissue Organ Printing (ITOP) system for simultaneously deposing inner and outer layers using GelMA bioink [11]. Further example is the study of Gao et al. in which alginate bioink was extruded and partially cross-linked at the same time. The material was deposited in a solution bath for permanently cross-linking the hydrogel. The results of the study are significant as they lead to the development of structure with high structural integrity [12]. Similar approach is presented by Han et al. Here, a compound of PVA and rubber elastomeric polymer was extruded as an outer layer and then dissolved in water for forming a mesh. The mesh structure had multipurpose; one supporting the tubular graft and second one, enabling curved shape. Subsequently, cell laden fibrinogen bioink is extruded from the inner nozzle while thrombin, cross-linker is pushed from the outer one [13]. Another innovative aspect of bio-printed hydrogel is the Freeform Reversible Embedding of Suspended Hydrogel (FRESH) technique. The approach is derived from extrusion-based bio-printing and focuses on deposing hydrogel in a viscous bath. The idea is to provide support for the deposition of low viscous bioinks. Initially Highly et al. used chemically modified hyaluronic acid (HA) at variating concentration, 25% for the dispensable hydrogel and 40% for the supporting matrix. The carefully selected concentrations were chosen after series of rheological tests that proved the bath's shear-yielding behavior and the rapid phase transition of the bioink [14]. Two months later, Bhattacharjee et al. have proved the method's effectiveness, by printing complex vascular three-dimensional network using polyvinyl alcohol (PVA) [15]. A month after Hinton et al. used gelatin microparticles for 3D printing series of complex geometries [16]. Additional techniques are adopted from other domains and derived to bio-printing. Such are inkjet based, laser and stereolithography (SLA). For instance Christensen et al. tried to spatially orient droplets of alginate with mouse fibroblast for initiating the formation of vascular branches with complex geometries [17]. Similarly, Wu et al. remarkable work included line deposition using biological laser processing/printing (BioLP) of human vein endothelial cells (HUVEC) and human umbilical vein smooth muscle cells (HUVSCMC) to observe the vessel formation [18]. SLA efforts persist to pioneer the field. Sodian et al. aimed to create a vascular segment for descending aorta replacement using polyglycolic acid (PGA) [19]. While 3D printing had made significant contribution to the field, various biofabrication processes are basing on traditional techniques. A perfect example is the one of Zhou et al. where they fabricated 3D thermoplastic mold using Fused Deposition modeling. The hydrogel, sodium alginate was initially pipetted to the mold,

while the cross-linking agent was introduced secondly. The constructs underwent in vitro testing, revealing remarkable cell viability rates of up to 90% [20].

In conclusion, many efforts are put for the development of transplantable artificial blood vessel, however a fully functional vascular construct has not been achieved so far. The bounds of the field lie in mimicking the complex vessel anatomy on such a small scale. Even though studies have provided three-layered scaffolds there are still anatomical mismatches from the human vessels in terms of layer thickness. This significant anomaly might cause pressure gradients that can grow into more severe consequences. Moreover, efforts are also put on improving inter-layer interactions, however taking into consideration of that cells livable matter, tissue function is temporarily obtained. Therefore, the scope of.

this work concentrates on the development of two innovative approaches for fabricating 3D scaffolds applied in blood vessel tissue engineering. The objective of this study is to observe the process capabilities of molding technique and a modified additive manufacturing approach. Once results are obtained, the constructs are evaluated in terms of dimensional accuracy and strain at break, then compared. The significance of this research is in the attempt to fabricate small diameter constructs (< 6 mm) with high precision and mechanical strength within the ISO 7198 for minimizing anatomical mismatches.

Materials and Methods

Materials

In this study two naturally obtained biopolymer Gelatin G9391, sourced from bovine skin and Alginate (A2033) extracted from algae were purchased from Merck group. Gelatin, a biopolymer derived from collagen through partial hydrolysis, contains twenty amino acids. While the amino acids are connected by strong covalent bonds, they interact through hydrogen, Van der Waals, electrostatic and hydrophobic bonds. These weak interaction play a crucial role in material's viscoelastic behavior as they brake easily at slightly increased temperature (operating temperature 10 °C – 40 °C) [21]. Gelatin is an excellent material as it is biocompatible and biodegradable, however it lacks in mechanical stability and therefore, it was mixed with alginate [22]. Similarly, alginate is biocompatible and biodegradable. However, unlike gelatin, alginate, provides parts with higher structural integrity. Yet, in general is often mixed with gelatin as its molecular chain lacks RGD groups which are necessary for cell adhesion. Hence, a blend of the two is commonly used to achieve a hydrogel with ideal mechanical and adhesive properties.

Hydrogel Prpearation

Gelatin and alginate powder mass was weighed corresponding to the predetermined concentration. In parallel, the solvent volume is pipetted into glass cup and placed on the stirrer at 40 °C. When the ionized water obtains the temperature, small volumes of alginate are added progressively until it is fully dissolved. Gelatin is poured in the same manner right after full dissolution of the first solute. The solution is then mixed for 3 h at the defined temperature. After, it is transferred to falcon tube and centrifuged at 23 °C for 40 min at 2900 rpm. Lastly, it was placed in the fridge for 40 min for stabilizing.

Method

Biofabrication of 3D Constructs

The idea of this study was to develop techniques for fabricating 3D constructs of small diameters. The first method involved a 3D prototyped bioprinter that translates with x–y-z coordinates and system that involves the rotation of a metal cylinder (Fig. 1).The method was inspired by the research team of Revoek-T [23].

The angular motion consisted an assembly of DC motor connected to a L298N Dual Channel H bridge and a power supply. The motor driver is then wired to Arduino (UNO) microcontroller that determines the motor function (Fig. 2). The motion is transmitted to the rod by attaching it to the motor with a 3D printed transition piece. The other side of the cylinder is fixed 3D printed support structure (Fig. 3).

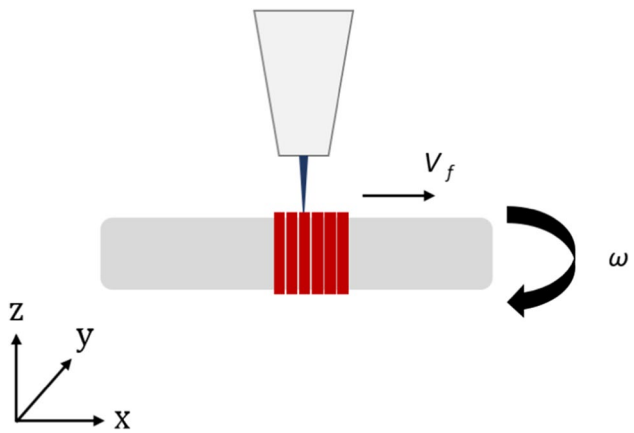

Fig. 1 Working principle of the prototyped model; V_f – extrusion speed, ω – angular velocity of the cylinder

The motion synchronization is based on the translation of the 3D printer's head and the rotation of the cylinder. In other words, while the extruder deposits material by displacing in the x – axis, the cylinder rotates. The objective is to perfectly align the two simultaneous motions so a helix is created over the rod. To do that one must first understand their relationship. If the two motions are constant, the pitch between each turn is constant (Fig. 4a). Similarly, if printer moves at a steady velocity while the rod accelerates, the f-distance reduces (Fig. 4b). Consequently, if the motor deaccelerates the cylinder while the extrusion head displaces continuously, the pitch increases (Fig. 4c).

Finding the relationship between the two motions implied the development of a formula that was based on a theory of bead circularity. First, one can postulate that a homogenous layer can be obtained only when the beads are tangential. Additionally, assuming perfect bead circularity, that indicates that the diameter of the bead equals the diameter of the needle ($d_{bead} = d_{needle}$). Therefore, the distance between two beads centers should equal one bead diameter (Fig. 5).

One can analytically express the flow rate (Q) as function of the bead's cross section and the translational motion (V_f) with following the formula:

$$Q = AV_f \tag{1}$$

However, the flow rate does not only depend on the translational velocity but as well as the angular velocity. T and thus, to find the relationship between the two, one must first assume that uniform flow rate is obtained once the beads' distance (f) equals the bead's diameter (d). This further

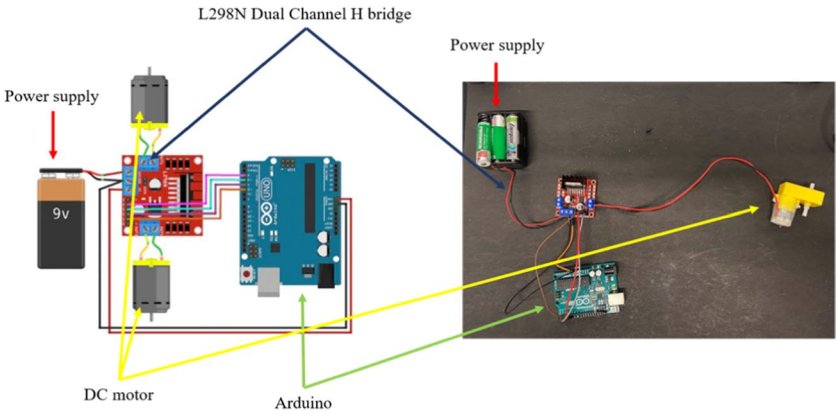

Fig. 2 System assembly

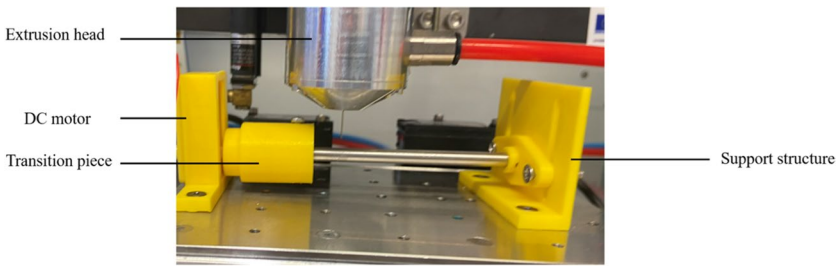

Fig. 3 Fixation of the prototyped system on the extrusion based system

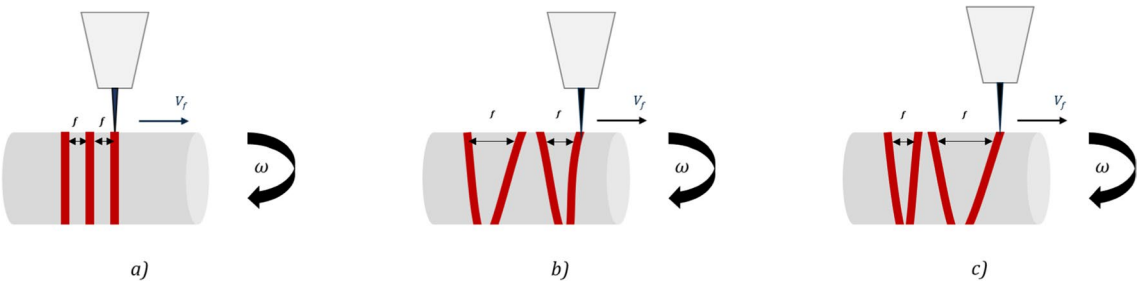

Fig. 4 The effect of velocity on the pitch f – pitch distance; V_f – velocity of the extruder; ω – angular velocity a) constant pitch distance due to constant velocities) pitch reduction due to acceleration c) pitch increase due to deacceleration

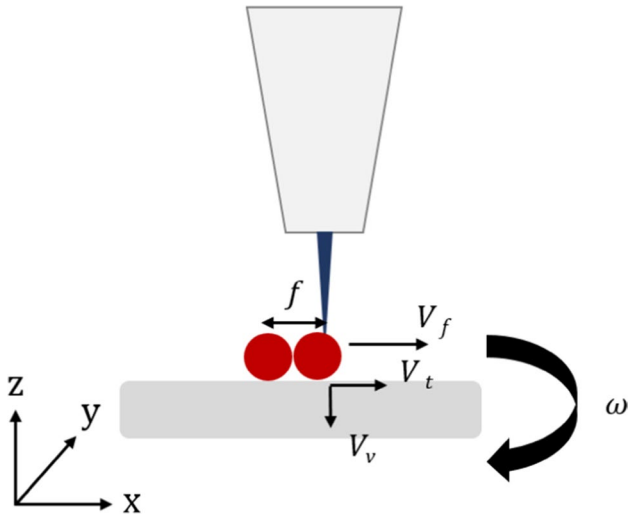

Fig. 5 Theory behind the relationship between the angular and translational motion on the bead diameter f – beads' pitch; ω – angular velocity composed of V_t- tangential component and V_v – vertical component; V_f—translation velocity

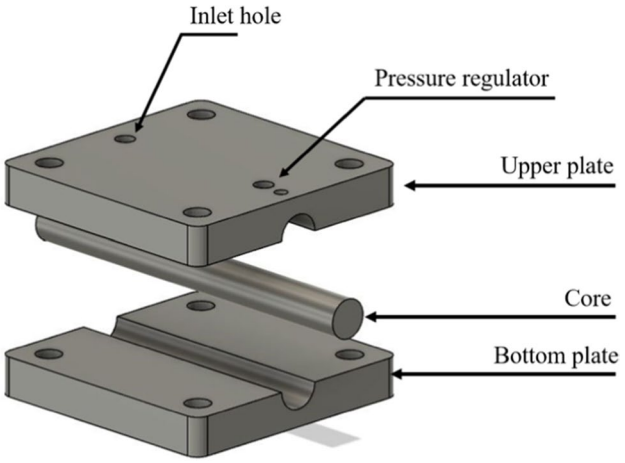

Fig. 6 Perspective view of the mold design

implies that Vf = Vt. Once the hypothesis is postulated, one can express the dependence of the two motions as a function of the beads' distance as expressed in the following:

$$f = V_f/\omega \tag{2}$$

where ω – angular velocity and V_f – translational velocity and equivalent with Vt.

Once the cylinder was fabricated, the rod was detached and placed in a 3% $CaCl_2$ solution for 20 min. This time was sufficient enough to cross-link the alginate. The solidified tubular structure was then removed and cut in three sections. Photos were taken of each section.

The following technique was based on the principle of injecting the fluid hydrogel into PLA (polylactic acid) mold. The mold was additively manufactured using a Cartesian 3D extrusion system, Ultimaker S5. Several experimental values were tested, before the final parametric set up was defined.

Prior to the experiments, trials were performed to confirm the functionality of the mold. The mold was composed of two halves assembled with screws. The interior of each part was dented with one semi-channel, and when they were put together, a complete channel was formed. The core with a smaller diameter than the channel, was placed in the cavity,. The offset two was filled with the material using 1 mL pipette. The mold with encapsulated hydrogel was left inside 3% $CaCl_2$ solution for cross linking (Fig. 5). There were multiple time intervals that were tested before the cross-linking was achieved.

Once the material was cross-linked it was extracted from the mold, divided in three thirds. Photos were taken of their cross section to measure the wall thickness and the diameter of the sample Fig. 6.

Elongation Test

Following ISO standard 7198, the obtained 3D cylinders from both, molding and 3D printing were manually elongated until break. The samples were clamped and then elongated using human effort until failure occurred. The strain was then calculated from the measured initial (Fig. 7a) and extended length (Fig. 7b).

Results

The experiments started by generating the G-code for the planned toolpath. Once the extruder was set, the motor was programmed, the motions were determined using Eq. 2. Additional preliminary experiments were executed for confirming the speed alignment. In the end, for 0.4 mm/s extrusion speed, the motor was set to rotate at 45 bits. Temperature and pressure were other parameters that were set to be constants, 23 °C and 3.5 bars respectably. The nozzle diameter corresponded to 0.25 mm. Once the part was 3D printed, it was left to cross-link for 20 min. Then, the tubular construct was divided in three segments (Fig. 8).

The part transparency created some challenges when it came to the capturing the results using microscopy. Thus, three thin slices were cut from each sample and measurements were taken with ImageJ. Each segment provided with two measurements for inner and outer diameter while thickness values were taken from four points (Fig. 9).

Three 3D constructs were fabricated and consequently, nine slices were measured. In the end, an average value was taken and compared with the theoretical one (Fig. 10).

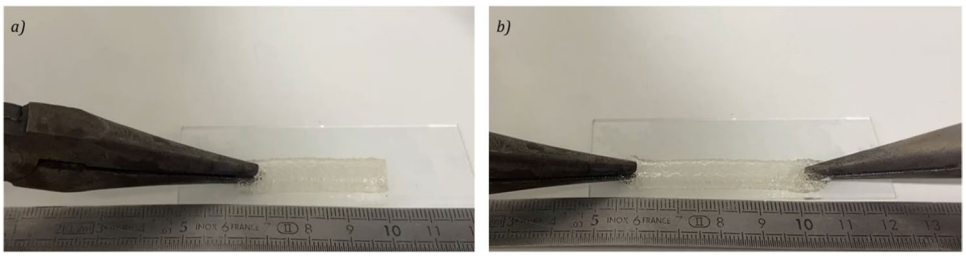

Fig. 7 Manual strain at break test a) Initial length b) extended length

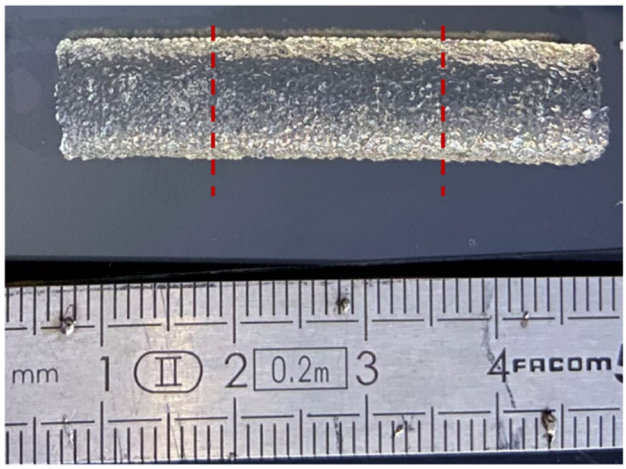

Fig. 8 Result of 3D printed construct; division in three sub-parts

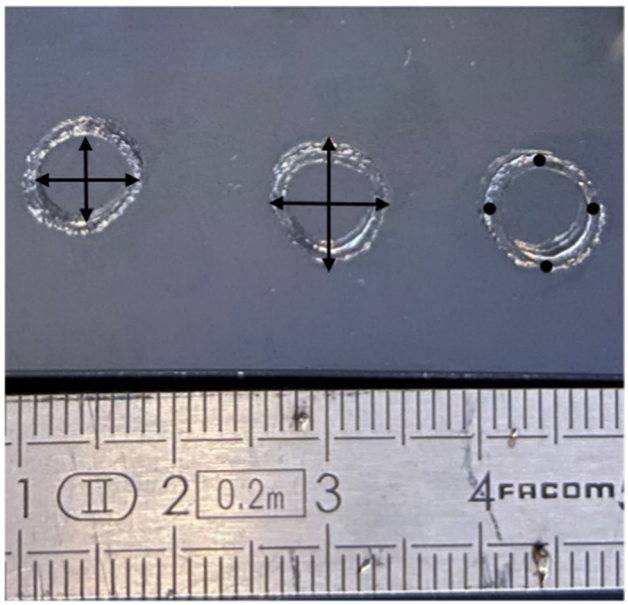

Fig. 9 Segments of the sliced 3D construct; left – example of how the inner diameter was measured; middle – demonstration of extracting values for the outer diameter; right – illustration of the points at where thickness values were taken

The theoretical values included: the thickness equivalent to the nozzle diameter (0.25 ± 0.1) and inner diameter of $6\,mm \pm 0.2$ (same as the diameter of the rod) and an outer diameter that was set to be the inner one plus two times the layer thickness ($6.6 \pm 0.2\,mm$).

The results of the molding technique were organized in the same manner as in bioprinting. Initially, the diameter of the semi-channel was set to be 6.5 ± 1 mm, 7 ± 1 mm and 7.5 ± 1 mm to form a wall thickness of 0.25, 0.5 or 0.75 mm. However, trials failed in all cases, as the offset was significantly small the material was not able to distribute over the mold. Finally, a diameter of 8 ± 1 mm was 3D printed for 1 ± 0.1 mm thickness. The results are presented in Fig. 11.

Once the measurements were taken, additional trials were stretched manually until break. The results are presented in Fig. 12. In the end, the maximum strain was found in percentage.

Discussion

The comparison of molding and 3D bioprinting took different turn than expected as trials of 0.25 mm thickness were not feasible. However, a parallel was made between the two techniques (Fig. 13).

Data of 3D printed construct show that while the outer diameter has an error of 11.5%, the one of the wall thickness deviates between 15.9 -24.3%. One assumption was made, based on the fact that the 3D printed construct was directly exposed to water, which lead to significant construct's expansion. However, considering the fact that the scaffold experiences retraction over 24 h period of time, one can estimate the waiting time to minimize this effect. Another solution can be to reduce the flow rate over the extrusion in order to optimize the wall thickness. To do that, one can develop a control and monitor system based on artificial intelligence to adjust the parameters during the process [24]. Molded constructs on the other hand, showed superior results as the defects corresponded to 0.94% for the outer diameter and within 6.42–12.32% range for the wall thickness. Consequently, following a coherent and rational sequence these characteristic can be assigned to the limited

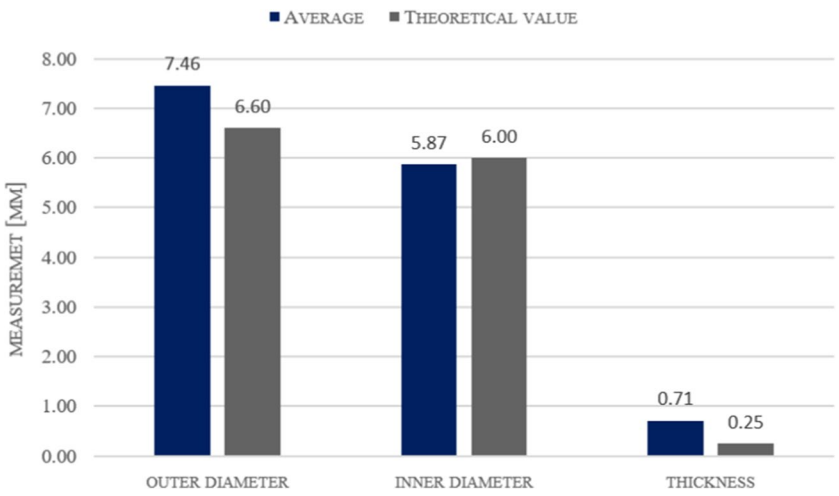

Fig. 10 Results of 3D spiral based technique; left column – comparison of the average value and the theoretical (expected) value of the outer diameter ($6.6 \pm 0.2\,mm$); middle column – expression of the average experimental value and the theoretical one ($6 \pm 0.2\,mm$); right column – correlation between the mean value obtained empirically and the theoretical one

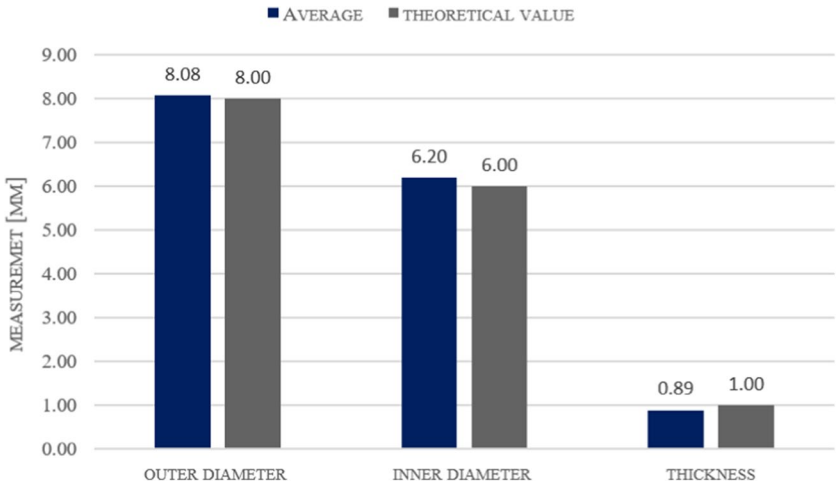

Fig. 11 Results from molding technique expressed in mm; right column – comparison between average experimental and theoretical outer diameter for range of 8 ± 1 mm; middle column – correlation of the theoretical and the mean inner diameter obtained experimentally ($6 \pm 1\,mm$); right column – thickness comparison ($range\ 1 \pm 0.1\,mm$)

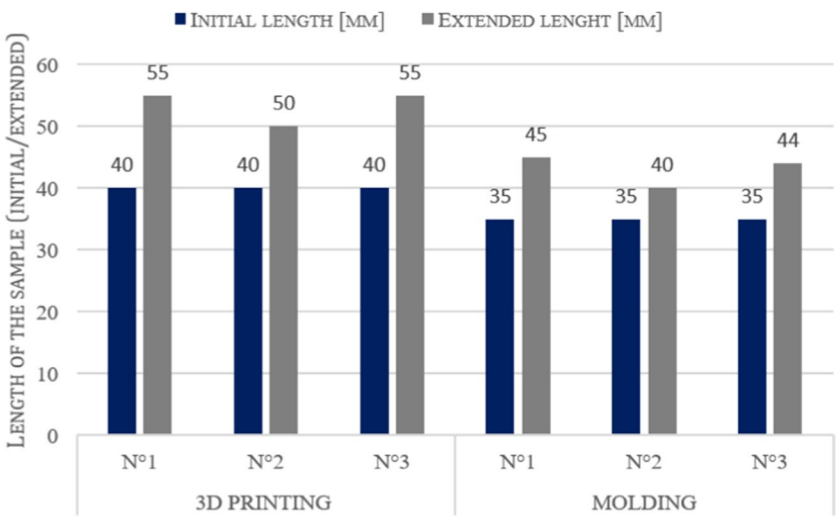

Fig. 12 Strain comparison between 3D spiral bioprinting and molding; left side – three bioprinted samples with $L_{initial} = 40$ mm were extended to 50 mm – 55 mm; right side – three molded experiments with $L_{initial} = 35$ mm and maximal extended one of 45 mm

water contact that restricted the water absorption. Another significant observation were surface properties. While 3D printed parts showed rougher surfaces, the molded ones had more integrated look (Fig. 14). However, there were certain zone of excessive material in the molding techniques that were removed using scalpel after the mold extraction. These zones were result of the inlet holes or the cavities that appeared between the plates.

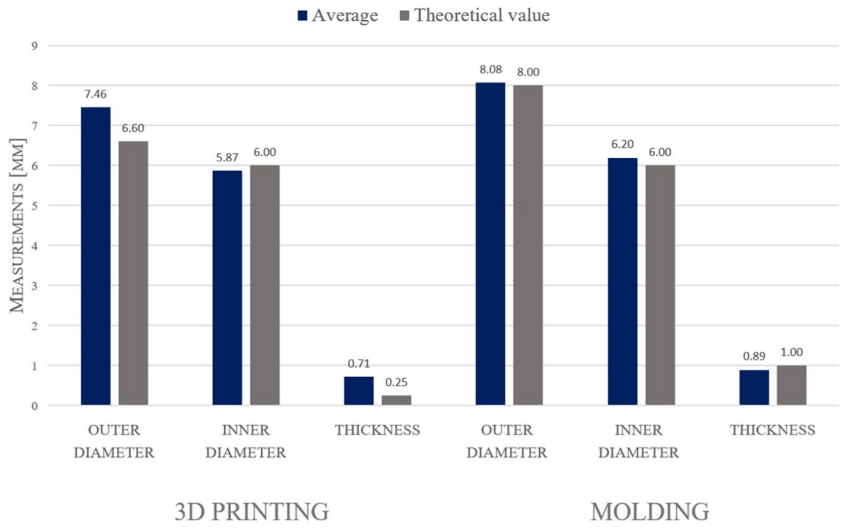

Fig. 13 Comparison between the measured values of 3D printing and molding; left– 3D spiral based bioprinting shows the mean values of the experimentally obtained diameter do not fit in the 6.6 ± 0.2 mm range, similarly the thickness average thickness obtained does not satisfy the tolerance criteria ($0.25 \pm 0.1\,mm$), while the inner diameter fell within the acceptable criteria ($6 \pm 0.2\,mm$); right side – molded samples mostly satisfied the criteria as the average outer diameter obtained was within 8 ± 1 mm, the inner diameter and the thickness were not completely satisfying the tolerance criteria, however the results were favorable

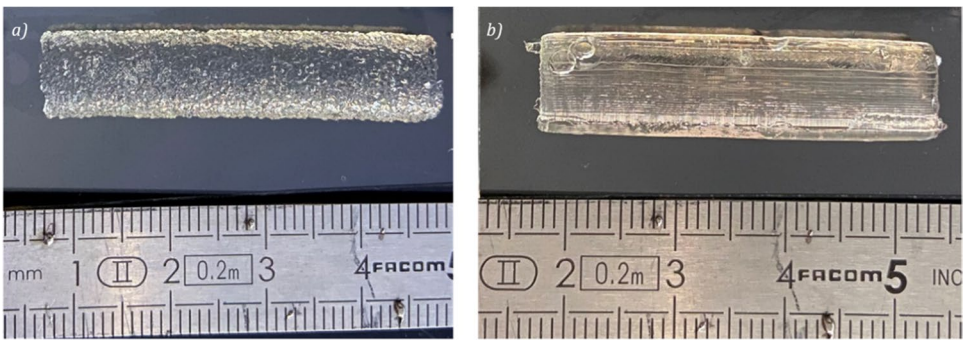

Fig. 14 Comparison between the 3D printed (a) and molded (b) construct. Visual assessment of the physical properties

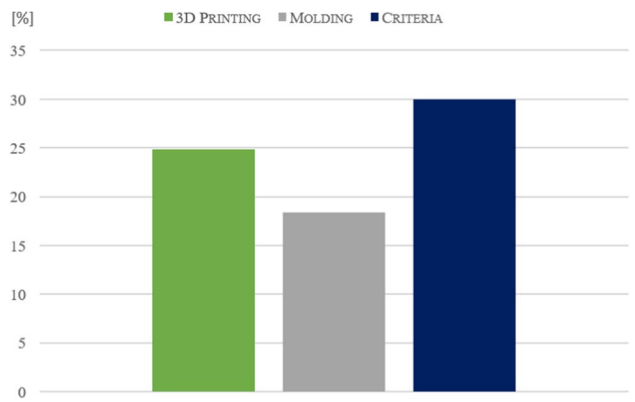

Fig. 15 Comparison between the two technique and the ISO 7198 standard; green column – the average strain obtained with spiral 3D printing (25%); grey column – the average experimental strain of molded parts (18%); blue column – ISO 7198 standard that defines the minimal strain to be 30%

Figure 15 shows the average extension at break for six samples, three 3D printed and three molded. The findings indicate that two out of three samples in 3D printing obtain a strain of 27%, while the average strain is approximately at 25%. These data are significant as they prove proximity to the ISO 7198. On the contrary, molded parts showed strain with average value of 18%, which does not satisfy the criteria. However, one must consider that the material properties are not considered in this tests. Therefore, the tests should be validated with Dynamical Mechanical Analysis (DMA).

Conclusion or Summary

In conclusion samples were first fabricated, then sectioned and measured using ImageJ. The data obtained was used for extracting the average value for the inner, outer diameter and the wall thickness. The results revealed that molding exhibited superior physical properties since the outer diameter fell within the admissible tolerance range of 8 ± 1 mm. Although the mean experimental values for the inner diameter and thickness did not fully meet the criteria, with a diameter of 6.2 mm (± 1 mm) and a wall thickness of 1 mm (± 1 mm), the variations were considerably small. The additive manufacturing approach on the other hand resulted in significant variations in terms of thickness considering that the experimental samples resulted in 0.71 mm for determined theoretical value of 0.25 ± 0.1 mm. Similarly the mean 7.46 mm outer diameter did not fit the criteria of 6.6 ± 0.2 mm. The one dimension that fell into the tolerance spectrum was the inner diameter of 5.87 mm experimental value for 6.0 ± 0.2 mm. These results demonstrate the difficulties of fabrication of 3D constructs with small diameters. However, considering that the most important role in layer interaction and cell migration is the wall thickness, molding technique showed promising outcome.

Another experimental set up was developed for evaluating the strain at break using manual clamping approach. Here, the AM approach surpassed the one of molding as two out of three tests were extended to 27% strain. This results is significant as it approaches to the 30% value defined by the ISO 7198 standard for characterizing vascular grafts. In contrast to this, molding samples did not reach the criteria as two out of three samples demonstrated strain of 22%, while the third one was 12%. This particular criteria sets the AM method in the lead.

All in all the findings express the advantages and limitations of the application of AM methods and molding within tissue engineering. Even though the objective was to produce samples with maximal accuracy and mechanical strength within the admissible criteria, one must not neglect the fact that the difficulties in engineering 3D blood vessels of small diameters. Therefore, this research outlined the capabilities of the techniques and further work will focus on implementing new solution for improving precision, layer uniformity and mechanical strength.

Acknowledgements This work was supported by Ecole Centrale Nantes.

Declarations

Conflicts of Interest The authors declare that they have any conflicts of interest related to the work in this paper.

References

1. British Heart Foundation (2023) Global heart & circulatory diseases factsheet
2. Muthiah V, George AM, Turco JV, Fuster V, Roth GA (2022) The global burden of cardiovascular diseases and risk. J Am Coll Cardiol. https://doi.org/10.1016/j.jacc.2022.11.005
3. World Health Organization (WH0) (2021) Cardiovascular diseases (CVDs). https://www.who.int
4. Saptarshi B, Patrick M (2016) Sydney ringer: the pipe water of new river water company and the discovery of the elixir of life. American College of Surgeons
5. Hu K, Li Y, Ke Z, Yang H, Lu C, Li Y, Guo Y, Wang W (2022) History, progress and future challenges of artificial blood vessels: a narrative review. Biomater Transl. https://doi.org/10.12336/biomatertransl.2022.01.008
6. Bom S, Ribeiro R, Riberio HM, Sanots C, Marto J (2022) On the progress of hydrogel-based 3D printing: correlating rheological properties with printing behavior. Int J Pharm. https://doi.org/10.1016/j.ijpharm.2022.121506
7. Naghieh S, Sarker MD, Sharma NK, Barhoumi Z, Chen X (2020) Printability of 3D printed hydrogel scaffolds: influence of hydrogel composition and printing parameters. Appl Sci. https://doi.org/10.3390/app10010292
8. Kang KH, Hockaday LA, Butcher JT (2012) Quantitative optimization of solid freeform deposition of aqueous hydrogel. Biofabrication. https://doi.org/10.1088/1758-5082/5/3/035001
9. Kokol V, Pottathara YB, Mihelčič M, Perše LS (2021) Rheological properties of gelatin hydrogels affected by flow-and- horizontally-induced cooling rates during 3D cryo-printing. Colloids Surf A Physicochem Eng Asp. Elsevier. https://doi.org/10.1016/j.colsurfa.2021.126356
10. Soltan N, Ning L, Mohabatpour F, Papagerakis P, Chen X (2019) Printability and cell viability in bioprinting alginate dialdehyde-gelatin scaffolds. ACS Biomater Sci Eng. https://doi.org/10.1021/acsbiomaterials.9b00167
11. Xu L, Varkey M, Jorgensen A, Ju J, Jin Q, Park JH, Fu Y, Zhang G, Ke D, Zhao W, Hou R, Atala H (2020) Bioprinting small diameter blood vessel constructs with an endothelial and smooth muscle cell bilayer in single step. Int Soc Biofabrication. https://doi.org/10.1088/1758-5090/aba2b6
12. Gao Q, He Y, Fu JZ, Liu A, Ma L (2015) Coaxial nozzle-assisted 3D bioprinting with build-in microchannels for nutrients delivery. https://doi.org/10.1016/j.biomaterials.2015.05.031
13. Hann SY, Cui H, Chen G, Boehm M, Esworthy T, Zhang LG (2022) 3D printed biomimetic flexible blood vessel with iPS cell-laden hierarchial multilayers. Biomed Eng Adv. https://doi.org/10.1016/j.bea.2022.100065
14. Highley CB, Rodell CB, Burdick JA (2015) Direct 3D printing of shear-thinning hydrogels into self-healing hydrogels. Adv Mater. https://doi.org/10.1002/adma.201501234
15. Bhattacharjee T, Zehnder SM, Rowe KG, Jain S, Nixon RM, Sawyer WG, Angelini TE (2015) Writing in the granular gel medium. Sci Adv. https://doi.org/10.1126/sciadv.1500655
16. Hinton TJ, Jallerat Q, Palchesko RN, Park JH, Grodzicki MS, Shue HJ, Ramadan MH, Hudson AR, Feinberg AW (2015) Three-dimensional printing of complex biological structures by freeform reversible embedding of suspended hydrogels. Sci Adv. https://doi.org/10.1126/sciadv.1500758
17. Christensen K, Xu C, Chai W, Zhang Z, Fu J, Huang Y (2015) Freeform inkjet printing of cellular structures with bifurcations. Biotechnol Bioeng. https://doi.org/10.1002/bit.25501
18. Wu PK, Ringeisen BR (2009) Development of human umbilical vein endothelial cell (HUVEC) and human umbilical vein smooth muscle cell (HUVSCM) branch/stem structure on hydrpgel layers

via biological laser printing. Biofabrication. https://doi.org/10.1088/1758-5082/2/1/014111
19. Sodian R, Fu P, Lueders C, Szymanski D, Fritsche C, Gutberlet M, Hoerstrup SP, Hausmann H, Lueth T, Hetzer R (2005) Tissue engineering of vascular conduits: fabrication of custom-made scaffolds using rapid prototyping techniques. Thorac Cardiovasc Surg. https://doi.org/10.1055/s-2005-837536
20. Zhou L, Li Y, Tu Q, Wang J (2023) A 3D printing mold method for rapid fabrication of artificial blood vessel. https://doi.org/10.1016/j.colsurfa.2023.130952
21. Wang X, Ao Q, Tian X, Fan J, Tong H, Hou W, Bai S (2017) Gelatin-based hydrogels for organ 3D bioprinting. Polymers. https://doi.org/10.3390/polym9090401
22. Ahmady A, Samah NH (2021) A review: gelatine as a bioadhesive material for medical and pharmaceutical applications. Int J Pharm. https://doi.org/10.1016/j.ijpharm.2021.121037
23. Benedict (2016) Monkeys undergo successful 3D printed blood vessel transplant in major stem cell biotech breakthrough. https://www.3ders.org
24. Vidal L, Hascoet N, Kavrakova T, Garcia AJ, Chinesta F, Hascoet JY (2022) Machine learning-based predictive model for printability and shape fidelity in biofabrication. In Tissue engineering part A 28:226–226